JOURNAL OF MATERIALS SCIENCE 32 (1997) 1249–1259

A transformation toughening white cast iron

S. K. HANN, J. D. GATES
Department of Mining and Metallurgical Engineering, The University of Queensland, St Lucia, Brisbane 4072, Australia

An experimental white cast iron with the unprecedented fracture toughness of 40 MPa $m^{1/2}$ is currently being studied to determine the mechanisms of toughening. This paper reports the investigation of the role of strain-induced martensitic (SIM) transformation. The dendritic microconstituent in the toughened alloy consists primarily of retained austenite, with precipitated M_7C_3 carbides and some martensite. Refrigeration experiments and differential scanning calorimetry (DSC) were used to demonstrate, firstly, that this retained austenite has an ''effective'' sub-ambient M_s temperature and, secondly, that SIM transformation can occur at ambient temperatures. Comparison between room temperature and elevated temperature K_{Ic} tests showed that the observed SIM produces a transformation toughening response in the alloy, contributing to, but not fully accounting for, its high toughness. SIM as a mechanism for transformation toughening has not previously been reported for white cast irons. Microhardness traverses on crack paths and X-ray diffraction (XRD) on fracture surfaces confirmed the interpretation of the K_{Ic} experiments. Further DSC and quantitative XRD showed that, as heat-treatment temperature is varied, there is a correlation between fracture toughness and the volume fraction of unstable retained austenite.

1. Introduction

The abrasion resistance of high-chromium white cast irons makes them attractive for applications in the mining industry. The microstructural characteristics determining their wear resistance have been investigated extensively [1–4]; however, their low fracture toughness has constrained them to service applications in which only limited amounts of impact occur.

Developmental work at The University of Queensland has been aimed at improving the fracture toughness of white cast irons by alloy modification and heat treatment. By reducing the carbon content and applying an unusually high-temperature heat treatment (1130 °C), an alloy has been developed with a fracture toughness of 40 MPa $m^{1/2}$ [5]. This is compared with 24–30 MPa $m^{1/2}$ typical of conventionally heat-treated high-carbon white irons. Hereafter, the phrase "the 1130 °C treated iron" will be used to denote the reduced carbon alloy heat treated for maximal fracture toughness.

In common with conventional high-chromium white cast irons, the microstructure of the reduced carbon alloy consists of primary dendrites and a continuous eutectic. In the as-cast condition, the dendrites remain fully austenitic to room temperature. The eutectic microconstituent is a continuous network of chromium-rich carbide and eutectic austenite which has at least partially transformed to martensite upon cooling from the melt. In order to increase the hardness it is normal to heat treat at temperatures around 1000 °C. At these temperatures, chromium-rich carbides precipitate from the austenite in the dendrites. This destabilizes the austenite so that upon subsequent cooling it transforms fully or partially to martensite.

The stability of austenite is a function of the concentrations of carbon and chromium in solution in the austenite, with higher concentrations depressing the M_s temperature. In the as-cast condition, the dendritic austenite is highly supersaturated with carbon and chromium, sufficient to depress M_s to well below room temperature. The thermal activation provided by heat treatment allows precipitation of chromium carbides, resulting in an increase in M_s to above room temperature and consequent transformation to martensite upon cooling. (The high degree of supersaturation in the as-cast condition must be due to kinetics: the low driving force for nucleation at high temperatures and the slowness of diffusion at lower temperatures. Nucleation presumably occurs at the lower temperatures, and heat treatment provides the thermal activation required for these nuclei to grow. Regardless of how high a heat-treatment temperature is used, there is always less carbon in solution after treatment than in the as-cast state [6].) The extent of the transformation is dependent upon the positions of the M_s and M_f temperatures relative to room temperature. Equilibrium solubility increases with temperature, so higher heat-treatment temperatures are expected to result in an increase in the ratio of retained austenite to martensite.

0022–2461

The influences of retained austenite in the dendritic constituent on the wear resistance and fracture toughness of high chromium cast iron have been debated in the literature. Retained austenite reduces the bulk hardness and might therefore be expected to reduce abrasion resistance. Some authors have found, however, that retained austenite actually improves abrasion resistance, reportedly due to its work-hardening properties [7–9]. While it has been suggested that substantially austenitic as-cast microstructures have a higher fracture toughness than substantially martensitic heat-treated microstructures [10, 11], the effect of dendritic microstructure on fracture toughness has not been studied explicitly [5], and the mechanisms by which toughness might be influenced by retained austenite are not well understood. Under impact–fatigue and combined impact–abrasion conditions, the effects of retained austenite are ambiguous, with findings ranging from beneficial [8, 12], through neutral [13], to detrimental [14–18].

Retained austenite in a structure may be highly stable, or may be unstable and susceptible to strain-induced transformation to martensite (SIM). The tendency for SIM around crack paths and adjacent to wear surfaces in chromium white irons containing retained austenite has been reported [3, 8, 12, 19, 20]. It has been suggested that SIM may be the mechanism underlying severe spalling of alloys with high proportions of retained austenite under impact-fatigue conditions [8]. However, the question of whether this mechanism has any influence on the fracture toughness of these alloys has not previously been addressed.

The work reported in this paper is an analysis of the occurrence of SIM, and its influence on the toughness, in the 1130 °C-treated white cast iron alloy.

2. Transformation toughening – an overview

Transformation toughening is a mechanism for toughening of materials commonly associated with ceramics and TRIP (transformation induced plasticity) steels. Experimental observations have shown that the stress field associated with crack initiation triggers a martensitic phase transformation in a zone which extends ahead of the crack tip. This is called the frontal zone. After the crack passes through the frontal zone, a steady-state zone is established which includes both the transformation ahead of the crack tip and a transformed component in its wake [21]. The consequence of this transformation is to increase the overall toughness of the material [22–24]. Increases in resistance to crack propagation associated with phase transformations may be due to one or more of the following possible mechanisms [25]:

(i) reduction in the local crack-tip stress intensity factor due to volume expansion in the crack wake (known as crack closure effects or crack shielding [21]);

(ii) dissipation of energy in the plastic zone by transformation shape strain;

(iii) dissipation of energy during crack propagation via crack-tip deflection.

It is possible that the transformation product may be inherently more brittle than the parent phase [24]. For transformation toughening to be effective in such cases it is a requirement that the toughening action of the transformation process must be more than that necessary to compensate for this effective embrittlement.

The fundamental requirement for any system to support one of the above mechanisms is that there exists a metastable phase within the microstructure that can transform martensitically to a second, more stable phase, under the influence of an applied stress. At a temperature known as M_s, the chemical free energy difference between the parent and product phases is equal to the critical chemical driving force for the martensitic transformation. It is possible for local stresses to provide an additional driving force so that transformation can occur at temperatures above M_s. If the sum of the chemical and mechanical driving forces exceeds the critical chemical driving force, then the transformation will occur. The magnitude of the mechanical driving force is a function of the applied stress and the orientation of the transformed phase.

In the case of iron alloys, two regimes in which this type of transformation can occur have been observed [26, 27], as shown in Fig. 1. In the lower temperature regime (between M_s and M_s^σ) the mechanical driving force required to trigger the transformation increases linearly with temperature. At temperatures above M_s^σ the linear relationship no longer holds and the mechanical driving force required to trigger the transformation is lower than that which would be predicted by extrapolating the line between M_s and M_s^σ. In this regime the decrease in critical applied stress corresponds to the plastic deformation of the parent phase. In the lower temperature regime, the transformation is

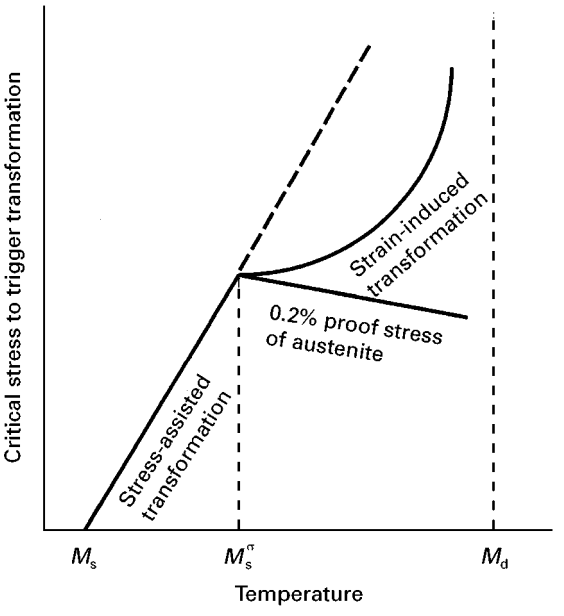

Figure 1 Schematic representation of the relationship between critical stress to trigger transformation and temperature above M_s. M_s^σ is the temperature above which the linear relationship between temperature and stress required to trigger transformation no longer holds. The corresponding value of stress required to trigger transformation at M_s^σ is equivalent to the yield point of the parent phase.

denoted "stress-assisted" while in the higher temperature regime it is denoted "strain-induced" [26]. There is a temperature, M_d, above which no martensitic transformation will occur at any level of applied stress. In fact, deformation of the parent phase above the M_d temperature has been shown to have a stabilizing effect, depressing the M_s temperature which will be measured upon subsequent cooling [25]. The temperature difference between M_s and M_d is dependent upon alloy composition. Values ranging from $\sim 80\,^{\circ}C$ (Fe–Ni–C alloys) to $\sim 440\,^{\circ}C$ (Fe–Mn–C alloys) have been recorded [28].

In summary, the basic requirements for transformation toughening of materials under stress at room temperature are that:

1. the M_s temperature of the parent phase be below ambient (this might apply only to a portion of the parent phase if there is compositional variation within it);
2. M_s be sufficiently near to room temperature to permit either stress-assisted or strain-induced transformation under the stress field around a crack; and
3. the transformation should result in crack closure, energy dissipation or another mechanism sufficient to give a net increase in fracture toughness.

3. Aims and methodology

3.1. Aims

The purposes of this investigation were:

(i) to establish whether transformation of the austenite to martensite can be triggered by the stress field associated with a propagating crack;

(ii) to investigate the possibility that this mechanism could be a factor contributing to the overall fracture toughness of the experimental alloy;

(iii) to investigate the effect of heat treatment on the M_s temperature and on the magnitude of the transformation.

(iv) Compare the observed trends with fracture toughness.

3.2. Strategy

With the aforementioned requirements for transformation toughening in mind, the following strategy was formulated.

(a) By using optical microscopy, to seek evidence of surface upheaval on polished and cryogenically treated specimens that would indicate the existence of a sub-ambient M_s temperature of the parent phase. To establish optically whether transformation is limited to either the eutectic or the dendritic microconstituent. To consider both the $1130\,^{\circ}C$-treated and the as-cast conditions.

(b) By using differential scanning calorimetry (DSC), to establish the *effective* M_s and M_f temperatures of the retained austenite phase. (The M_s temperature of the destabilized austenite is the temperature at which martensitic transformation starts upon cooling from the heat-treatment temperature. In cases where the M_f is below room temperature, the transformation will not go to completion and some austenite will be retained. The "effective" M_s is defined as the temperature at which this retained austenite will begin transforming upon subsequent cooling below room temperature. As some stabilization of the retained austenite may occur as a consequence of the arrest in transformation by room temperature, this effective M_s temperature may be substantially less than room temperature.) Also, to measure the enthalpy of the transformation. Consider both the $1130\,^{\circ}C$-treated and the as-cast conditions.

(c) In the case of the $1130\,^{\circ}C$-treated iron, to establish whether a martensitic transformation of the retained austenite can be triggered at room temperature under the influence of mechanical deformation (applied by impact). To measure the magnitude of any remaining thermal transformation using DSC.

(d) To test the fracture toughness of the alloy in both the $1130\,^{\circ}C$-treated and as-cast conditions at room temperature (RT). To look for evidence of SIM in the crack wake by examining the fracture surfaces and crack paths of the tested fracture toughness specimens.

(e) To estimate the M_d temperature of the transformation. (This estimate would be based on the position of M_s obtained from the DSC result above and the difference between M_s and M_d typical of materials reported in the literature.) To test the fracture toughness of the alloy in both the as-cast and $1130\,^{\circ}C$-treated condition using an elevated test temperature (ET) which is above the estimated M_d. To compare the fracture toughness data from the RT and the ET fracture toughness tests, and to draw conclusions regarding the contribution of any transformation toughening mechanism operating in the alloy.

(f) By examining the fracture surfaces and crack-paths of the ET fracture toughness specimens, again to look for evidence of SIM in the crack wake. In this way, to check for any tendency of the crack-tip stress field to trigger a SIM transformation at the elevated temperature.

(g) To determine the effect of heat-treatment temperature on both the toughness and the transformation properties by conducting a series of DSC and XRD retained austenite measurements. To compare these results with the variation in fracture toughness with heat treatment presented by Kootsookos *et al.* [5].

3.3. Experimental procedure

3.3.1. Microstructural evaluation

The hypoeutectic alloy investigated had the following composition: Fe–1.86C–18.2Cr–1.9Mo–1.5Ni–1.2Si–1.1Mn–1.0Cu. Specimens in both the as-cast and $1130\,^{\circ}C$-treated conditions were used in the analysis. Heat treatment was carried out for 4 h at temperature followed by air cooling to room temperature. Specimens were then subcritically treated (tempered) for 2 h at $200\,^{\circ}C$ and air cooled to room temperature.

3.3.2. Optical microscopy and differential scanning calorimetry

Specimens were polished but not etched. These were imaged optically under interference contrast conditions. The dendrite structure was clearly visible under these conditions due to pronounced relief polishing effects caused by the large discrepancies between the hardness of the eutectic carbides and the dendrites in these alloys. The specimens were then cryogenically treated by immersion in liquid nitrogen and inspected for evidence of transformation-induced surface upheaval.

Specimens from both the as-cast and the 1130 °C-treated conditions were prepared for differential scanning calorimetry (DSC) from ~500 μm thick slices with surfaces ground to 600 grit to ensure good platen contact area. As only melting point data were available for the standards, the DSC was calibrated in the heating mode using indium and dodecane. However, scans were run in the cooling mode. A scan rate of $-40\,^{\circ}C\,min^{-1}$ from 0 °C to −140 °C was used for all tests. Owing to the non-reversible nature of the martensitic transformation, it was possible to obtain base-line correction data by re-heating specimens to room temperature and repeating the initial run at the same rate. Using this technique the need to run a standard specimen in parallel for base-line calibration was avoided.

3.3.3. K_{Ic} fracture toughness testing

K_{Ic} single-edge notched beam (SENB) three-point bend specimens were tested in accordance with ASTM E-399. Specimens from both the as-cast and the 1130 °C-treated alloys were tested at room and elevated (135 °C) temperatures. Specimens were notched using a combination of abrasive cutting and electric-discharge machining. The small-root radius of the final notch reduced the time taken for initiation of fatigue pre-cracks. Fatigue pre-cracks were established at the root of the notch using a servo-hydraulic Instron mechanical testing machine under computer control. This technique allows the crack length and growth rate to be constantly monitored and adjusted during the pre-cracking operation. In all cases, fatigue pre-cracking was conducted at room temperature. Fracture toughness tests were conducted using a servo-hydraulic Instron machine and load versus crack opening displacement curves were obtained using a chart recorder. A Welwyn clip gauge, capable of operating at elevated temperatures up to 230 °C, was used for all tests including those conducted at elevated temperature.

In the evaluation of the transformation toughening characteristics of other materials, some authors have elected not to use crack opening displacement (COD) gauges for their immersion bath-type elevated temperature tests [24]. In the present study, however, COD data were collected during all fracture toughness tests to ensure consistent results were obtained.

The testing temperature selected for the ET tests was an estimate of a temperature exceeding the predicted M_d. Specimens for ET fracture toughness testing were wrapped in multiple layers of "Kaowool" insulating material with only the loading points exposed, and oven heated to a temperature slightly in excess of the required testing temperature. Specimens were then removed from the oven and tested immediately. The temperature drop after removal from the oven of the insulated specimens was measured using a thermocouple. After 4 min had elapsed the total temperature drop was less than 10 °C. All ET fracture toughness tests were completed within a total elapsed time of less than 4 mins.

After fracture toughness testing, DSC scans were run to ensure the sub-ambient martensitic transformation characteristics were consistent from specimen to specimen. Specimens for DSC were prepared from each of the 1130 °C-treated fracture toughness bars. This also provided a secondary check to ensure the transformation characteristics of the material were unaffected by the elevated fracture toughness testing temperature.

3.3.4. Microhardness measurements

Microhardness measurements of specimens taken from the 1130 °C treated and as-cast fracture toughness bars were made in order to determine the extent of the transformation that occurred during crack growth. Both the RT and ET K_{Ic} tests were interrupted after the peak load had been obtained in order to preserve the double-sided crack paths for microstructural evaluation. Cross-sections from the central plane strain region of the crack path from each of the K_{Ic} test bars were mounted, polished and lightly etched (Fig. 2). Vickers' microhardness measurements were made using a 100 g indentor load which provided an indent size small enough to be contained within the dendrites. Dendritic hardness measurements were made along traverses perpendicular to the crack direction. Measurements were taken at approximately

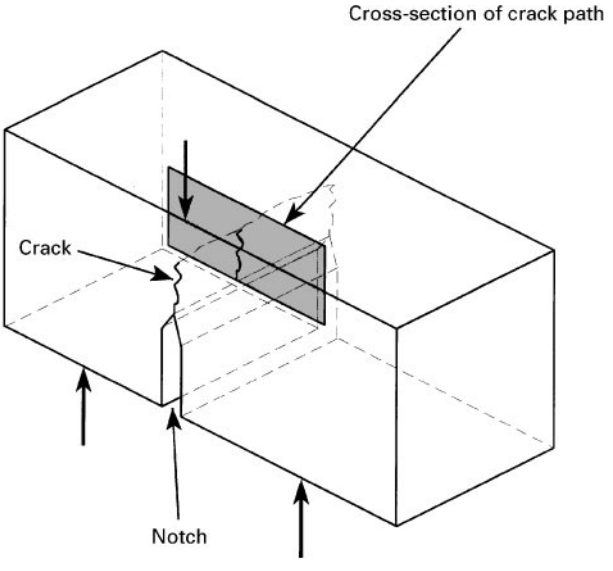

Figure 2 Schematic drawing of SENB fracture toughness bar. The shaded plane represents the cross-section used for μH_V measurements.

50 μm intervals to a distance of 1000 μm. Data from at least five traverses ensured that potential interference from eutectic carbides below the indentor were minimized.

3.3.5. Qualitative X-ray diffraction

X-ray diffraction (XRD) scans were collected from the fracture surfaces retrieved from the fracture toughness specimens of the 1130 °C-treated alloy. Fracture surfaces of approximately 100 mm^2 were scanned through 2θ values ranging from 18°–48° to identify the phases present on or adjacent to the fracture surface. A sectioned and polished specimen of the 1130 °C-treated alloy was also scanned for comparison. MoK_α radiation was used, giving an average penetration depth for the scan range selected of approximately 15 μm. Results obtained are qualitative only, as no account of surface roughness or texturing effects was taken.

3.3.6. Variation in retained austenite with heat treatment (using XRD and DSC)

The variation in retained austenite with heat-treatment temperature was measured using XRD. Polished specimens were prepared from the following destabilization and tempering heat treatments: 1000 + 200 °C, 1050 + 200 °C, 1100 + 200 °C, 1130 + 200 °C and 1150 + 200 °C. Other than the variation in destabilization temperature all aspects of the heat-treatment conditions were the same as those previously described. Each specimen was scanned through 2θ values ranging from 26.5°–46°. After the initial scan, specimens were further treated by immersion in liquid nitrogen and subsequently rescanned under the same conditions. In this way it was possible to determine what fraction of the retained austenite was stable to below −196 °C. Traces were obtained using MoK_α radiation and a horizontal tilt/rotate goniometer. Data were collected on a Nicolet 4094 digital oscilloscope and smoothed using the Nicolet five-point averaging system prior to analysis. The Kim [29] method for calculation of the austenite to martensite ratio was used.

Specimens from the above heat treatments were also analysed using DSC. Specimen preparation, DSC calibration and scanning conditions were the same as those previously mentioned.

4. Results and discussion

4.1. Microstructure and the effect of cryogenic treatment

Optical microscopy indicates that in the as-cast condition, the primary dendrites of the reduced-carbon alloy are fully austenitic. Transmission electron microscopy (TEM) shows that the eutectic carbides are M_7C_3, while the eutectic austenite has transformed to martensite.

In the 1130 °C-treated condition, optical microscopy shows the precipitation of carbides within dendrites which otherwise appear to remain essentially austenitic. TEM shows that the precipitated carbides are M_7C_3 and that they are sheathed by martensite. Laths of martensite also extend from these sheaths into the surrounding matrix. Similar martensitic structures are also in evidence in regions adjacent to the eutectic microconstituent. The eutectic is unchanged from that in the as-cast microstructure. Examples of the as-cast and 1130 °C-treated microstructures are presented in Fig. 3.

After cryogenic cooling of the as-cast alloy, no changes were evident in the microstructure as revealed by conventional metallographic polishing and etching techniques. In order to verify this apparent lack of change, previously polished specimens were examined after cryogenic treatment in search of evidence of surface upheavals indicative of the shape strain associated with martensitic transformations. No such upheavals could be found, as shown in Fig. 4a and b. This indicates that the austenite in the as-cast condition is stable to temperatures lower than −196 °C.

The 1130 °C-treated specimen, by contrast, showed extensive upheaval of the surface after cryogenic cooling, as shown in Fig. 4c and d. These upheavals are strongly indicative of martensitic transformation within the dendrites. In both the as-cast and 1130 °C-treated conditions the eutectic microconstituent was unaffected by the cryogenic treatment. This result is consistent with the observation that the eutectic matrix is already fully transformed in the as-cast condition.

Differential scanning calorimetry (DSC) was used in order to quantify the transformation occurring upon cryogenic treatment. In the as-cast alloy there was no measurable transformation exotherm in the DSC scans, as shown in Fig. 5. This lack of transformation confirms the conclusion from the surface upheaval experiment, that the austenite in the dendrites is extremely stable.

DSC scans for the 1130 °C-treated alloy (Fig. 5) show a substantial exotherm from transformation to martensite. There is a distinct sub-ambient M_s temperature at between −10 and −20 °C. Subsequently, the amount of martensite formed increases with the degree of cooling below M_s, until the transformation process is complete at about −130 °C. The magnitude of the full transformation exotherm was measured to be 9.5 ± 2 J g^{-1}.

Deformation of 1130 °C-treated specimens prior to running DSC scans resulted in a marked reduction in the magnitude of the transformation exotherm (Fig. 6). The magnitude of this reduction increased with increasing amounts of plastic deformation. When sufficient plastic deformation was imposed, the measurable thermal transformation was reduced to zero. The relative position and shape of the exotherms from the lightly deformed specimens was, in other respects, unchanged from those occurring in the undeformed specimens.

4.2. K_{Ic} fracture toughness

The fracture toughness for the 1130 °C-treated alloy was measured to be 39 ± 2 MPa $m^{1/2}$. This agrees well

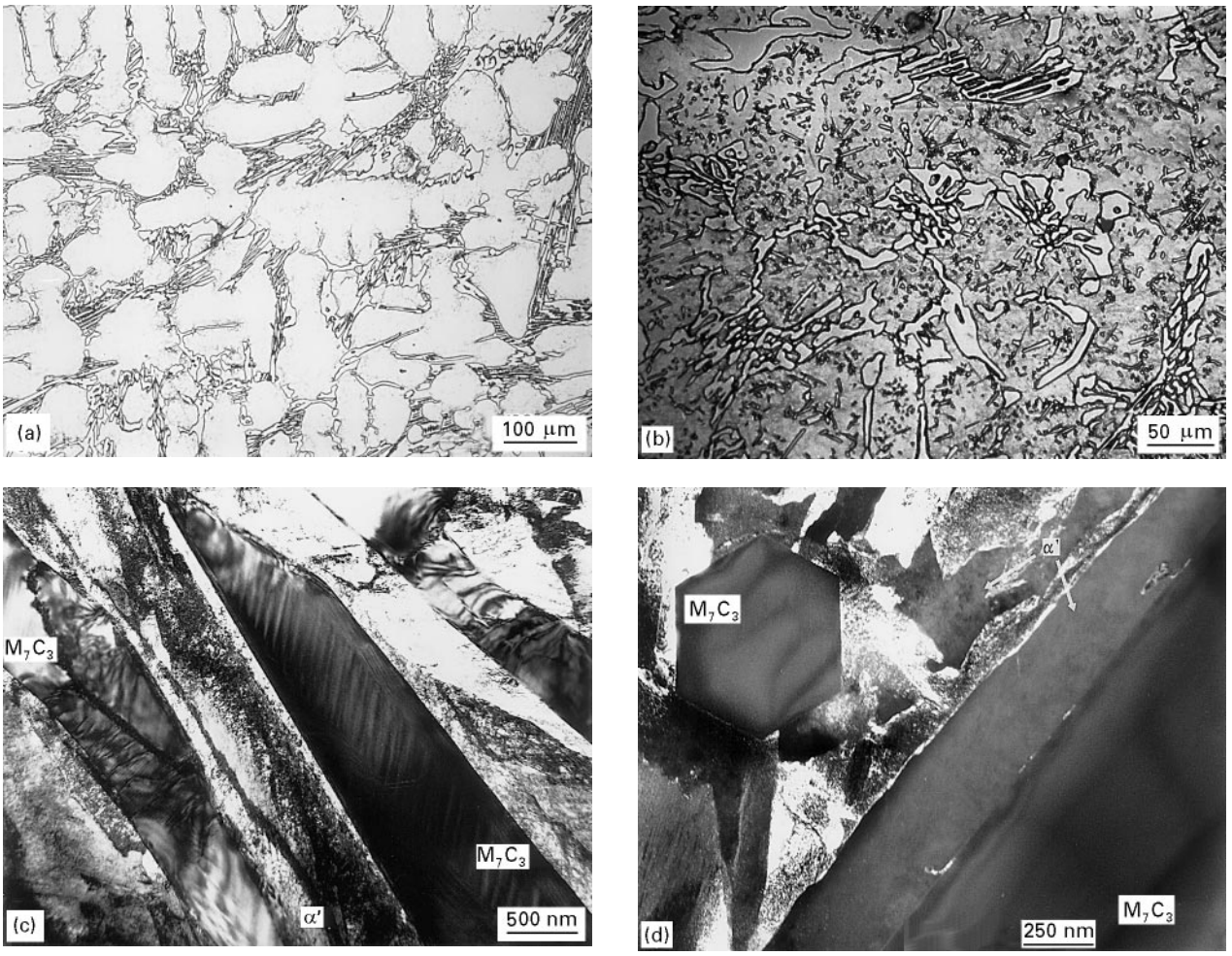

Figure 3 Optical and transmission electron micrographs of the as-cast and 1130 °C-treated microstructures. Selected-area electron diffraction was used for TEM phase identification. (a) As-cast alloy. (b) 1130 °C-treated alloy. (c) Transmission electron micrograph of the eutectic region of the as-cast alloy. M_7C_3 eutectic carbides and eutectic martensite are indicated. (d) TEM dark-field micrograph of the dendritic region of the 1130 °C-treated alloy. Note the precipitated M_7C_3 carbides and the surrounding martensite. (e) Transmission electron micrograph showing the microstructural detail of a region adjacent to a precipitated carbide in the dendritic region of the 1130 °C-treated alloy. Note the existence of martensite laths in the region immediately adjacent to the carbide that extend into the surrounding retained austenite.

with the value of 40 ± 2 MPa m$^{1/2}$ measured on this alloy by Kootsookos [5].

K_{Ic} data for the as-cast and 1130 °C-treated specimens are presented in Fig. 7. Error bars indicate the range of data obtained from the five specimens in each treatment. For the room-temperature tests the fracture toughness values for the 1130 °C-treated and the as-cast alloys were approximately 39 ± 2 and 30 ± 2 MPa m$^{1/2}$, respectively, a difference of about 9 MPa m$^{1/2}$. By contrast, in the case of the elevated temperature tests, the fracture toughness of the 1130 °C-treated and as-cast alloys were approximately 33 ± 2 and 30 ± 2 MPa m$^{1/2}$, respectively, a reduced difference of about 3 MPa m$^{1/2}$.

It would normally be expected that the elevated testing temperature would result in either no difference or perhaps a slight increase in fracture toughness due to increased plasticity effects. This expectation is borne out in the results for the as-cast material. The elevated testing temperature had little or no effect on the fracture toughness of the alloy, with 30 ± 2 MPa m$^{1/2}$ being measured at both test temperatures.

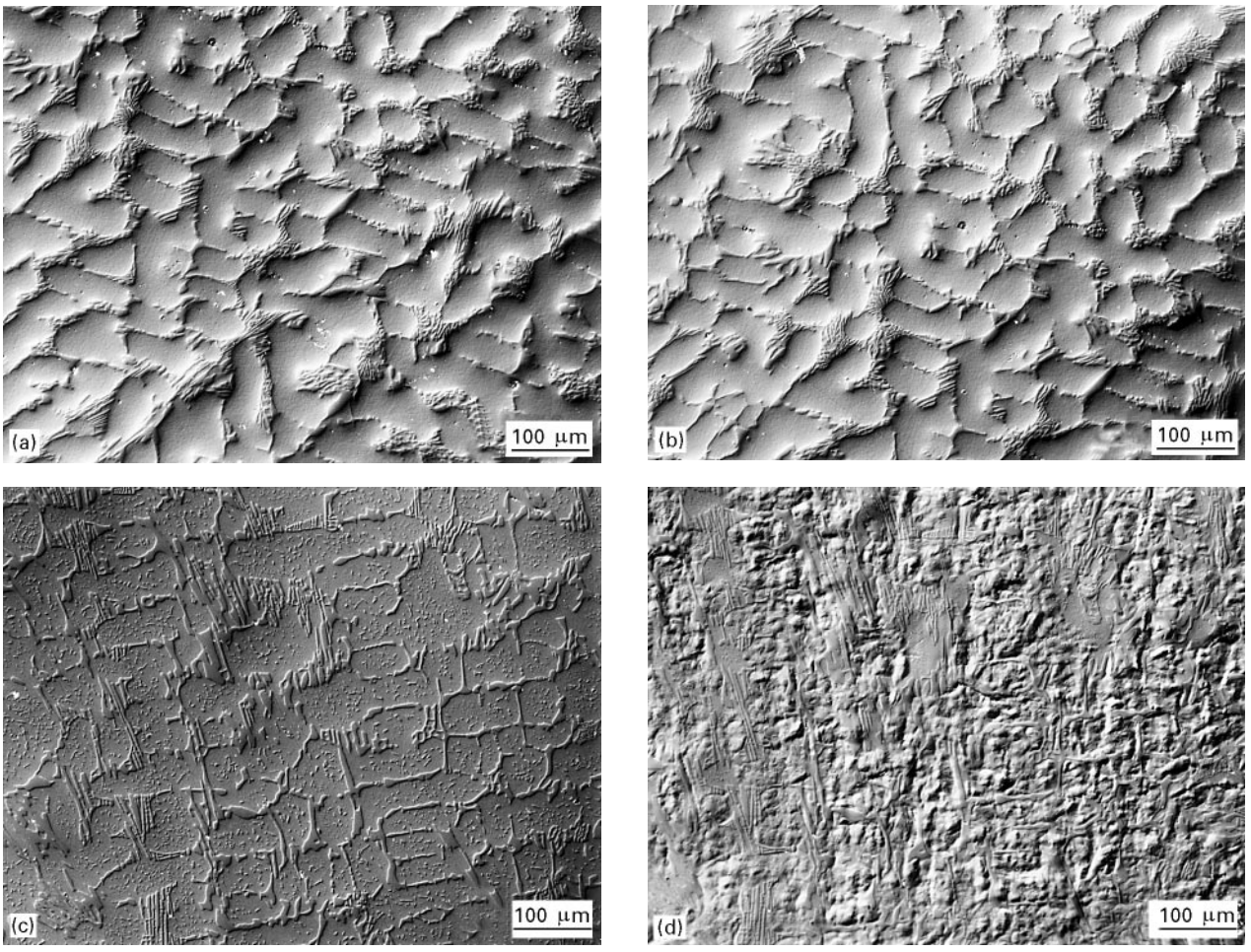

Figure 4 Optical micrographs from the as-cast and 1130 °C-treated alloy. Specimens were polished but not etched, with relief polishing effects being enhanced with the use of interference contrast microscopy. (a) General polished section of the as-cast microstructure. (b) The same region of the as-cast microstructure as featured in (a), after cryogenic treatment by immersion in liquid nitrogen. Dendritic regions are unaffected by cryogenic treatment due to the stability of the austenite. (c) General polished section of the 1130 °C-treated microstructure. (d) The same region as featured in (c) after cryogenic treatment. Note the pronounced surface upheavals as a consequence of martensitic transformation within the dendrites.

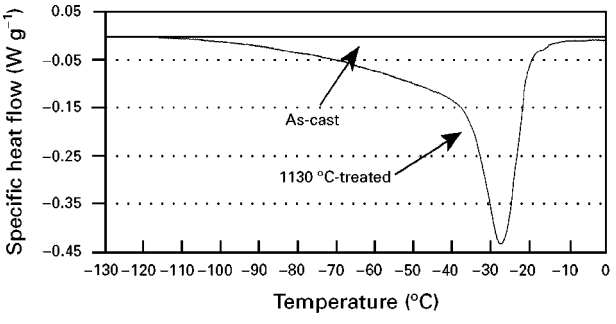

Figure 5 DSC scans showing the magnitude of the transformation exotherms for both the as-cast and 1130 °C-treated alloy.

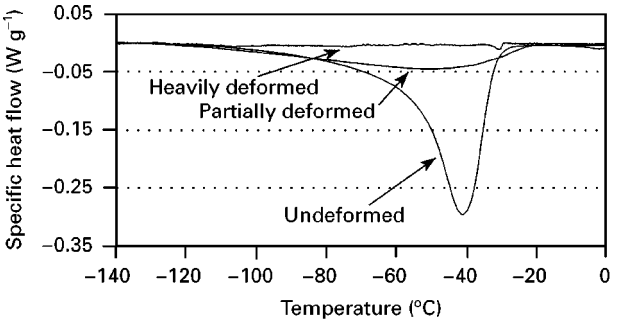

Figure 6 DSC scans showing the relationship between deformation and the size of the transformation exotherm for the 1130 °C-treated alloy.

In the case of the 1130 °C-treated alloy, however, the reverse trend was observed. A marked drop of about 6 MPa $m^{1/2}$ between the room temperature and the elevated temperature fracture toughness results was recorded. It is postulated that at room temperature, a portion of the total fracture toughness is attributable to the mechanism of transformation toughening. It is also postulated that at the elevated temperature the fracture toughness is a measure of the toughness of the material in the absence of this transformation toughening mechanism. It is consequently inferred that the difference of 6 MPa $m^{1/2}$ between the RT and ET tests is a measure of the contribution of transformation toughening to the overall toughness of the material.

4.3. Microhardness measurements

The above hypotheses are based on the assumption that the elevated testing temperature of 135 °C is in excess of the M_d temperature, thus preventing any strain-induced transformation from occurring. The

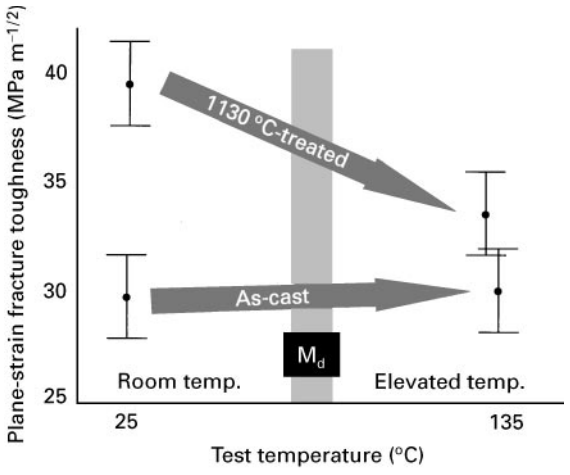

Figure 7 Showing the effect of testing temperature on the fracture toughness of as-cast and 1130 °C-treated specimens.

validity of this assumption was investigated by observation of the crack paths of the elevated temperature and room-temperature fracture toughness bars.

Fig. 8 shows the relationship between the dendritic microhardness and the perpendicular distance from the crack, measured on cross-sectional specimens from each of the K_{Ic} bars. For the 1130 °C-treated alloy tested at room temperature, there is a pronounced increase in hardness associated with the crack, with the hardness increasing from about 500 μHV in regions remote (>500 μm) from it to about 800 μHV within 50 μm of it. For the same material tested at elevated temperature there was no such dependence of hardness on distance from the crack. In this case the microhardness of the dendritic microconstituent was uniform at about 500 μHV which was equivalent to the value measured in undeformed specimens of the 1130 °C treated alloy.

In the as-cast alloy, a similar lack of dependence was found, in specimens tested at both room temperature and elevated temperature. The dendritic microhardness remained constant at about 360 μH_V, independent of distance from the crack. This value is lower than the undeformed hardness in the 1130 °C-treated alloy due to the presence of secondary carbides and some transformation products in the latter.

As the stability of the dendritic austenite in the as-cast alloy had already been established, the result that there was no measurable difference in the microhardness between the RT and ET crack paths was as expected. Any dependence of dendritic hardness upon distance from the crack would be attributable to conventional work hardening within the plastic zone. The observation that no such dependence occurred suggests that in the case of the 1130 °C-treated alloy any measurable difference in hardness with distance from the crack must be attributable solely to the presence of transformation products.

Hence, for the 1130 °C-treated alloy tested at room temperature the marked dependence of hardness upon distance from the crack indicates that significant transformation occurs in regions adjacent to the crack and that this effect extends a distance of approximately 500 μm into the material. For the

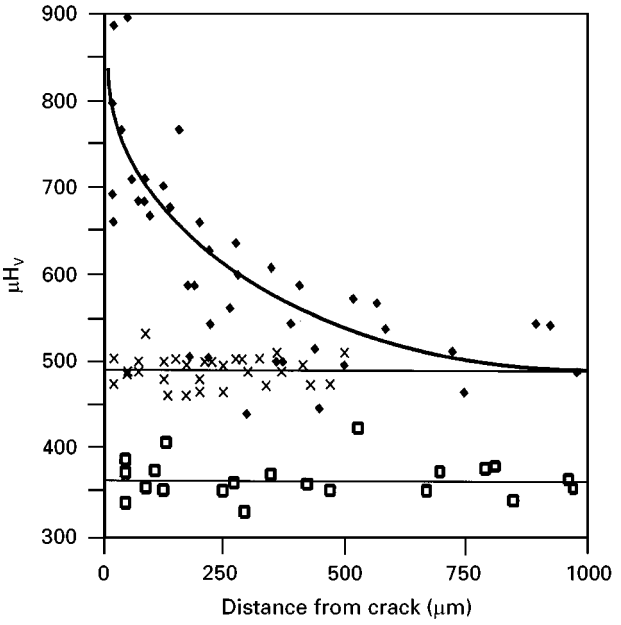

Figure 8 Variation of the dendritic microhardness with perpendicular distance from the crack. Specimens are cross-sections of the crack path from the (◆) RT and (×) ET fracture toughness bars, in the 1130 °C-treated alloy, and for (□) RT and ET tests in the as-cast alloy.

1130 °C-treated alloy tested at elevated temperature, the absence of any dependence of hardness on distance from the crack demonstrates that the testing temperature of 135 °C was in excess of M_d and that consequently no strain-induced transformation had been triggered.

4.4. X-ray diffraction

The polished specimens of the 1130 °C-treated alloy represent general cross-sections of the undeformed microstructure. XRD traces obtained from these specimens show clear evidence of both austenite and martensite phases, as expected (Fig. 9c). The presence of M_7C_3 reflections is somewhat less obvious, with some of the peak positions being shared with those of austenite. Other M_7C_3 reflections of similar intensity according to structure factor calculations are not visible at all. These predicted peak positions have been indicated on the axis of Fig. 9a. The absence of strong evidence of M_7C_3 carbide in the traces in general may be explained by the fact that carbide reflections occurring in this scan range represent high order planes that give low diffraction intensity.

XRD traces obtained from the fracture surfaces of the 1130 °C-treated alloy tested at elevated temperature also show evidence of austenite and martensite phases (Fig. 9a). In those obtained from the 1130 °C-treated alloy tested at room temperature, however, scans show strong reflections from martensite only (Fig. 9b), with austenite reflections absent.

As no account for specimen texturing has been taken in this analysis, it is not possible to draw conclusions about small differences in the relative proportions of the phases that are present. The complete absence of a phase in a scan, however, must be significant.

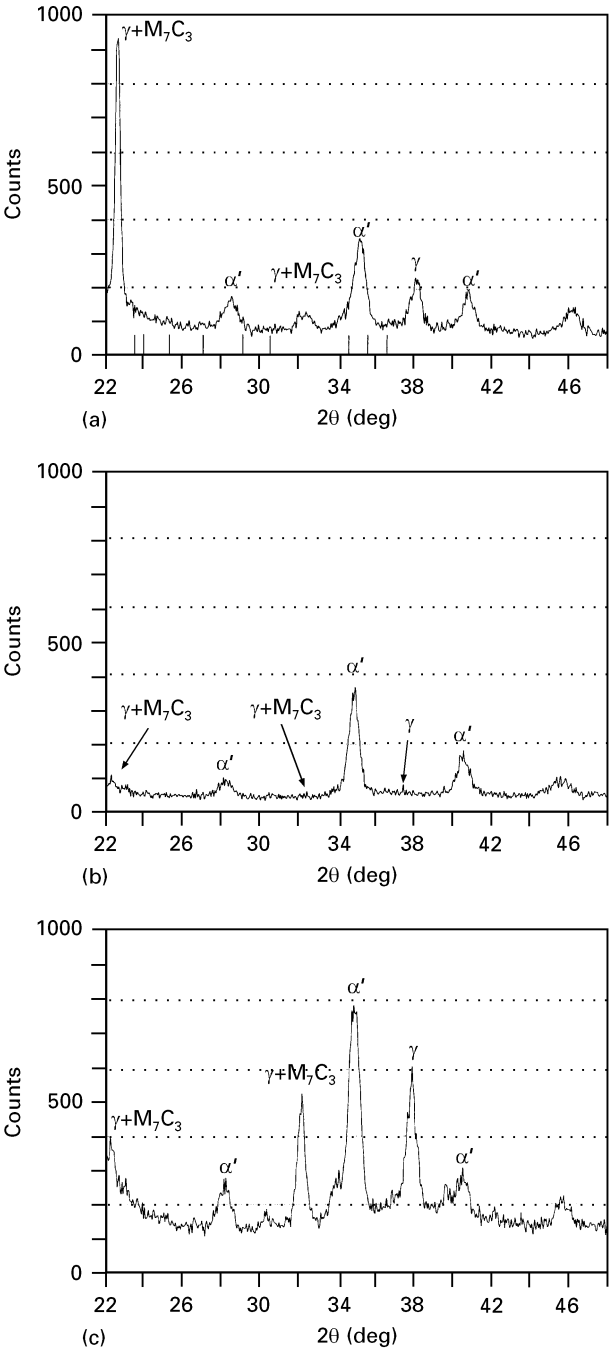

Figure 9 XRD scans from the 1130 °C-treated alloy. (a) Fracture surface of 1130 °C-treated K_{Ic} specimen tested at ET. (b) Fracture surface of 1130 °C-treated K_{Ic} specimen tested at RT. (c) General polished section of 1130 °C-treated alloy.

In the case of the specimens obtained from the fracture surfaces of the K_{Ic} bars it might be expected that if the crack path preferentially followed the eutectic microconstituent there would be little evidence of austenite appearing on the subsequent XRD traces. However, in the case of the 1130 °C-treated material tested at elevated temperature, austenite was clearly evident on the XRD traces, suggesting either that the penetration depth of the molybdenum radiation (about 15 μm) was enough to compensate this effect or that the crack path included propagation through the dendrites. In either case, the austenite was evidently not transformed by the stress field of the advancing crack.

Fractographic studies of the 1130 °C-treated alloy tested at room temperature have shown that the crack path includes both the dendritic and the eutectic microconstituents [30]. The observation that the XRD traces of the fracture surface of the 1130 °C-treated alloy tested at room temperature contained almost no evidence of austenite is further confirmation of the strain-induced transformation that occurs under the influence of an advancing crack. It is not known whether the crack path of the 1130 °C-treated alloy, when fractured at elevated temperature, is similar to that of the alloy when fractured at room temperature. It is intended that this be investigated, in an attempt to explain the observation that the 1130 °C-treated alloy tested at elevated temperature has a higher toughness than that of the as-cast alloy (Fig. 7).

4.5. Variation in retained austenite with heat treatment (using XRD and DSC)

A comparison was made between the results from both the XRD and DSC investigations and previously reported fracture toughness values for the alloy that were measured over the same range of heat-treatment temperatures [5].

The variation in fracture toughness of the alloy with heat-treatment temperature is presented in Fig. 10a. The toughness increases with increasing destabilization temperatures over 1050 °C until a maximum of 40 MPa $m^{1/2}$ is reached at about 1130 °C.

Fig. 10b shows the relationship between the magnitude of the DSC exotherm and the heat-treatment temperature over the same range of heat treatments. The trend is similar to that above, with the size of the exotherm increasing with heat-treatment temperature for temperatures above 1050 °C and reaching a maximum at about 1130 °C.

Fig. 10c shows the variation in austenite to martensite ratio with heat-treatment temperature measured using XRD. Curves showing "total austenite" to martensite ratio, AR_T, "stable austenite" to martensite ratio, AR_S, and "unstable austenite" to martensite ratio, AR_U, versus heat-treatment temperature are displayed on the same axes. AR_S represents the austenite that remained untransformed after the cryogenic treatment and $AR_U = AR_T - AR_S$. From these curves it can be seen that both the total volume fraction of retained austenite and the stable volume fraction of retained austenite increase with increasing heat-treatment temperature. For the unstable retained austenite it can be seen that the trend is the same as that of the DSC result, as expected, with the largest value of AR_U occurring at the 1130 °C heat-treatment temperature.

The close-matching forms of these three curves suggests that the fracture toughness of the alloy is dependent upon the amount of austenite that is susceptible to strain-induced transformation. It is this component of the retained austenite that affects the magnitude of transformation toughening possible in the material. The highest fracture toughness recorded here corresponds to the heat treatment resulting in the largest volume fraction of unstable retained austenite.

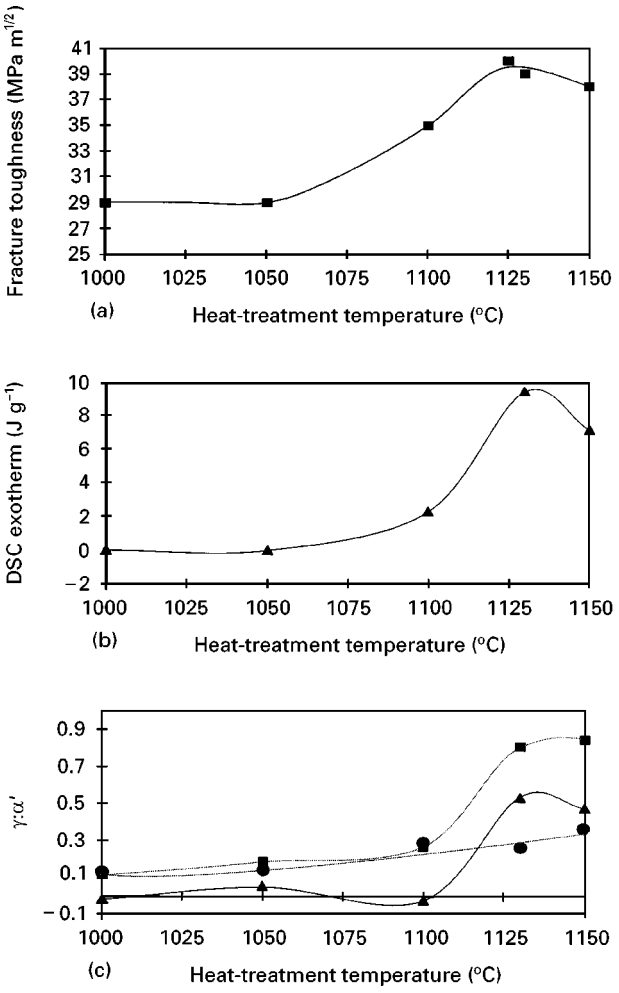

Figure 10 Dependence of various parameters on heat-treatment temperature. (a) Variation in fracture toughness with heat-treatment temperature, after Kootsookos [5] with data from the current study included. (b) Relationship between the magnitude of the DSC exotherm and the heat-treatment temperature over the same range of heat treatments. (c) XRD result showing the correlation between austenite to martensite ratio and heat-treatment temperature. (■) $AR_T =$ "total austenite" to martensite ratio; (●) $AR_S =$ "stable austenite" to martensite ratio; (▲) $AR_U =$ "unstable austenite" to martensite ratio $= AR_T - AR_S$.

Although the XRD traces for the 1130 °C-treated alloy show that some stable retained austenite exists at −196 °C, inspection of the individual DSC curves (Fig. 5) suggests that, in each case, the transformation appears to be complete at approximately −130 °C. It is also noted that the AR_S versus heat-treatment temperature curve (Fig. 10c) does not increase at a rate corresponding to the increase in the AR_T curve. Two possible interpretations of this behaviour are

(a) that the composition of the austenite in the destabilized microstructure is not uniform across the dendrites but rather is separated into at least two discrete regions. In one region the austenite has an M_s temperature close to room temperature and in the other the austenite is stable to temperatures below −196 °C;

(b) that due to the variation in composition of the austenite in the dendrites as a consequence of the heat-treatment temperature, the amount of austenite that will be retained after the cryogenic treatment correspondingly varies.

Microanalysis studies previously conducted on white cast irons have revealed that after high-temperature destabilization treatments, the composition of the dendrites is not uniform across their cross-section [31–33]. The existence of interlath-retained austenite is common to martensitic structures and is a function of both the carbon content and the amount of austenite stabilizing elements present [34]. This suggests that compositional variation in retained austenite between the heat treatments may result in different amounts of retained austenite after cryogenic treatment. Further microanalysis and TEM investigations are required to establish whether these transformation characteristics are a consequence of local segregation or bulk compositional variation.

5. Conclusions

1. The significant contribution of transformation toughening to the overall toughness of an experimental white cast iron has been demonstrated. The existence of this mechanism has not previously been reported for white cast irons.

2. DSC was shown to be a valuable tool for evaluation of the characteristics of sub-ambient martensitic transformations.

3. Further crack-path and microstructural studies are required to explain the component of toughening in the 1130 °C-treated alloy that could not be attributed to the transformation toughening mechanism.

Acknowledgements

The authors thank Dr Maurice Ripley, Australian Nuclear Science and Technology Organisation, Lucas Heights, Sydney for technical equipment support, and Mike Bosworth and Dr G. L. F. Powell, CSIRO Division of Manufacturing Technology, Adelaide, for XRD facilities. David Hunter, Department of Chemistry, The University of Queensland, is thanked for DSC facilities. This work was performed with funding from the Australian Research Council and Mount Isa Mines Limited.

References

1. J. LIU, S. LI and Y. MAN, *Wear* **166** (1993) 37.
2. J. D. GATES and R. A. EATON, *Mater. Forum* **17** (1993) 369.
3. J. T. H. PEARCE, *AFS Trans.* **126** (1984) 599.
4. J. D. WATSON, P. J. MUTTON and I.R. SARE, *Metals Forum* **3** (1980) 74.
5. A. KOOTSOOKOS, J. D. GATES and R.A. EATON, *Cast Metals* **7** (1995) 239.
6. J. D. GATES, R. SCHMIDT and A. KOOTSOOKOS (1991) unpublished microstructural observations.
7. S. TURENNE, F. LAVALLEE and J. MASOUNAVE, *J. Mater. Sci.* **24** (1989) 3021.
8. J.-M. TONG, Y-Z. ZHOU, T-Y. SHEN and H-J. DENG, *Wear* **135** (1990) 217.
9. H. S. AVERY, in "Proceedings of Materials for the Mining Industry", Vail, CO, edited by R. Q. Barr (Climax Molybdenum Company, 1974), p. 43.
10. I. R. SARE, *Metals Technol.* **6** (1979) 412.
11. K. H. ZUM GAHR and D. V. DOANE, *Metall. Trans.* **11A** (1980) 613.

12. A. SINATORA, M. POHL and E. U. WALDHERR, *Scripta Metall. Mater.* **32** (1995) 857.
13. I. R. SARE, B. K. ARNOLD, G. A. DUNLOP and P. G. LLOYD, *Wear* **162–164** (1993) 790.
14. J. DODD and J. L. PARKS, *Metal Forum* **3** (1980) 3.
15. R. BLICKENSDERFER, J. H. TYLCZAK and G. LAIRD II, in "Proceedings of Wear of Materials", Denver, 1989, edited by K. C. Ludema (The American Society of Mechanical Engineers, New York, 1989) p. 175.
16. J. Y. SU, Y. Q. CHEN and Q. D. CHEN, *Wear* **135** (1990) 391.
17. X. H. FAN, L. HE and Q. D. ZHOU, *ibid.* **138** (1990) 47.
18. J. T. XI, Q. D. ZHOU, S. H. LIU and G. S. SONG, *ibid.* **162** (1993) 83.
19. J. T. H. PEARCE, *ibid.* **89** (1983) 333.
20. R. W. DURMAN, *Br. Foundryman* **74** (1981) 45.
21. D. J. GREEN, R. H. J. HANNINK and M. V. SWAIN, "Transformation Toughening of Ceramics" (CRC Press, Boca Raton, FL., 1989).
22. R. M. McMEEKING and A. G. EVANS, *J. Am. Ceram. Soc.* **65** (1982) 242.
23. W. W. GERBERICH, P. L. HEMMINGS, V. F. ZACKAY and E. R. PARKER, in "Proceedings of Fracture 1969–The Second International Conference on Fracture", edited by P. L. Pratt (Chapman and Hall, London, 1969) p. 288.
24. S. D. ANTOLOVICH and B. SINGH, *Metall. Trans.* **2** (1971) 2135.
25. B. C. MUDDLE and P. M. KELLY, *Mater. Forum* **11** (1988) 182.
26. G. B. OLSON and M. COHEN, *J. Less-Common Metals* **28** (1972) 107.
27. G. B. OLSON and M. COHEN, in "Proceedings of Joint U.S.-Japan Conference on Mechanical Behaviour of Metals and Alloys Associated with Displacive Phase Transformations", Troy, New York, 1979 (Massachusetts Institute of Technology, Cambridge, Mass, 1979) p. 1.
28. G. B. OLSON and W. S. OWEN, (eds) "Martensite" (ASM International, Metals Park, Ohio, 1992).
29. C. KIM, *J. Heat Treat.* **1** (1979) 43.
30. A. KOOTSOOKOS, PhD thesis, Department of Mining and Metallurgical Engineering, The University of Queensland (1995).
31. P. DUPIN, J. SAVERNA and J. M. SCHISSLER, *AFS Trans.* **90** (1982) 711.
32. G. L. F. POWELL and G. LAIRD II, *J. Mater. Sci.* **27** (1992) 29.
33. P. N. CREPEAU and S.D. ANTOLOVICH, *AFS Trans.* **94** (1986) 503.
34. G. KRAUSS, "Steels: Heat Treatment and Processing Principals" (ASM International, Metals Park, Ohio, 1993).

Received 13 November 1995
and accepted 8 May 1996